Dynamics of Protein-Bound Water in the Heme Domain of P450BM3 Studied by High-Pressure Spectroscopy: Comparison with P450cam and P450 2B4[†]

Dmitri R. Davydov,[§] Gaston Hui Bon Hoa,[‖] and Julian A. Peterson*,[⊥]

Institute of Biomedical Chemistry, Moscow, Russia 119832, Institut de Biologie Physico-Chimique, INSERM Unité 310, Paris, France 75005, and Department of Biochemistry, The University of Texas Southwestern Medical Center at Dallas, Dallas, Texas 75235-9038

Received June 15, 1998; Revised Manuscript Received October 26, 1998

ABSTRACT: Pressure-induced transitions in the heme domain of cytochrome P450BM3 (P450BMP) were studied versus the concentration of palmitic acid. An increase in hydrostatic pressure causes a high- to low-spin shift and subsequent P450 to P420 transition. Conversion of P450BMP to P420 is associated with important conformational and hydration changes of the protein. Treating the pressure-induced changes in the high-spin content in P450 in terms of the four-state model of spin transitions and substrate binding, we evaluated and compared the barotropic parameters of these transitions for P450MBP, P450cam, and P450 2B4 (2B4). In the current study, the pressure-induced transitions in P450cam were reinvestigated versus the concentration of camphor. The interactions of 2B4 and P450BMP with their substrates (benzphetamine and palmitic acid) were accompanied by larger changes in the partial volume of the proteins (+267 and +248 mL/mol, respectively) than the interactions of P450cam with camphor (+106 mL/mol). For 2B4 and P450BMP, substrate binding apparently requires hydration of regions outside the active site. The reaction volumes of the low- to high-spin transitions of the substrate-free cytochromes (20−23 mL/mol) are consistent with the displacement of one water molecule. The volume changes in the high- to low-spin transition of the substrate-bound P450cam, 2B4, and P450BMP (−90, −49, and −16 mL/mol correspondingly) reveal a linear relationship with $\Delta G°$ of the spin transition, suggesting that modulation of the spin state by substrate binding is driven by a common mechanism in all three heme proteins.

Protein-bound water is extremely important for intermolecular interactions and conformational transitions (*1*−*6*). Study of the role of water in the reaction cycle of P450s initially focused on water as the replaceable sixth ligand of the P450 heme iron (*7*, *8*). NMR spectroscopic examination of the relaxation of bulk solvent protons by P450cam[1] in the absence and presence of the substrate camphor indicated first and most surprisingly that solvent protons were in rapid exchange with protons on a ligand of the heme iron (*7*). Distance calculations indicated that solvent protons exchanged with protons that were approximately 2.6 Å from the heme iron, indicating that water was the replaceable *Z*-axis ligand of the heme iron. Camphor binding blocked the rapid exchange of solvent protons consistent with displacement of the axial water molecule from the heme iron accompanied by the low- to high-spin transition of the iron (*7*). With the solution of the crystal structure of P450cam in both the substrate-free and substrate-bound forms, the presence of water as the *Z*-axis ligand of the heme iron in the absence of the substrate camphor was confirmed (*9*). Substrate binding resulted in displacement of the heme-bound water (*10*). The presence of water molecules in the active site and their role in the reaction cycle has been of continuing interest (*11*−*16*).

A very specific mechanism for the regulation of water access to the heme moiety by substrate binding was recently suggested for P450cam and P450BM3 (*17*). This mechanism involves the movement of the side chain of arg299 of P450cam (arg319 of BM3) between "open" and "closed" conformations. However, there is direct communication between the substrate binding site and bulk solvent over the I-helix past asp267 in molecule B of the P450BM3 dimer in the X-ray crystal structure (*18*). The analogous amino acid residue (asp251) in P450cam has been shown to participate in salt bridge-triggering of the substrate access channel and plays an important role in proton delivery and the catalytic cycle of this cytochrome (*19*−*21*). Substrate binding in P450cam is accompanied by changes in the arg186−asp251 and lys178−asp251 salt bridges as well as transient changes in protein hydration (*22*). Thus, the delivery of protons, via protein-bound water, to the heme moiety is important for preventing the uncoupling of the electron flow in cytochromes P450 (*14*). A detailed knowledge of the mechanism of proton delivery is necessary to understand the reasons for relatively low coupling in the eukaryotic monooxygenases (*23*) compared with their bacterial counterparts.

[†] This research was supported in part by a National Institutes of Health Research Grant GM43479 to J.A.P., a North Atlantic Treaty Organization Travel Grant SA 11-1-05-OUTREACH to J.A.P. and D.R.D., a Research Grant RFBR 97-4-49132 from the Russian Foundation of Basic Research to D.R.D., and INSERM Est/Ouest cooperation program (Contract 94EO3) to D.R.D. and G.H.B.H.

* To whom correspondence should be addressed. E-mail: Bill@P450BM3.swmed.edu.

[§] Institute of Biomedical Chemistry.

[‖] INSERM Unité 310.

[⊥] The University of Texas Southwestern Medical Center at Dallas.

[1] P450BMP, the heme protein domain of P450BM3, CYP102; P450cam, CYP101; P450 2B4, CYP2B4; and PCA, principal component analysis.

10.1021/bi981397a CCC: $18.00
Published on Web 12/19/1998

The displacement of the equilibrium of chemical reactions by hydrostatic pressure is widely used to determine reaction volume changes ($\Delta V°$) (*24*−*27*). Among the factors determining $\Delta V°$, the changes in the hydration of the reacting molecules play the most important role (*28*, *29*). The partial volume, $V°$, of a protein in solution can be approximately described by the sum of three terms, namely, the intrinsic molar volume, V_M, the "thermal volume", V_T, and the "interaction volume", V_I (*30*, *31*). The thermal volume may be thought of as an "empty" domain around the solute molecule resulting from mutual thermal motions, while the interaction volume represents the solvent volume change due to hydration that is determined by negative contributions from the solvent-exposed charged and polar surfaces of the solute, which cause adjacent water molecules to form a local tightly packed network (*32*, *33*). The combination of V_T and V_I reflects the fact that the volume occupied by water molecules is larger near apolar atoms on the protein surface and smaller near charged atoms, in comparison to "bulk" water molecules (*32*, *34*).

Recently Chalikian and Breslauer (*35*) have determined that, on average, the exposure of 1 Å^2 of hydrophobic surface of protein to the water phase results in an increase of the sum of the V_T and V_I terms by 0.67 mL/(mol·Å^2). In contrast, the average contribution of polar and charged surfaces to these terms was found to be equal to −0.47 mL/(mol·Å^2). Tightening of water packing near surface charges is known as "electrostriction" (*27*, *32*, *36*). The partial volume of electrostricted water is estimated to be about 15 mL/mol (*36*), which is 3 mL/mol smaller than the 18.1 mL/mol value characteristic for "bulk" water (*37*, *38*). Thus, hydrophobic hydration and electrostriction affect the density (partial molar volume) of bound water as compared to bulk solvent

Although V_T and V_I terms are very important in the volume changes in protein transitions, the changes in the intrinsic volume of the protein, V_M, cannot be neglected. These changes are due mainly to the changes in hydration of protein cavities, which are nearly always present in proteins greater than 100 residues in size (*39*). Changes in hydration of protein cavities often accompany the processes of protein−ligand and protein−protein interactions, especially if the cavity constitutes a part of the intermolecular interface (*4*, *5*, *40*, *41*).

The importance of protein-bound water in the catalytic cycle of P450-dependent monooxygenases has been examined for P450cam and P450 2B4 (*14*, *15*, *42*−*44*). Osmotic and hydrostatic pressure effects on substrate binding to P450cam (*11*, *13*, *15*) implicate more water molecules in this process than are found in the active site of substrate-free P450cam (*9*). Exposure of camphor-bound P450cam to high hydrostatic pressure was shown to cause a shift of the spin equilibrium toward the low-spin form. This transition is characterized by a $\Delta V°_{spin}$ in the range of −20 to −100 mL/mol, depending on the nature of the substrate and the experimental conditions (*11*, *13*). A decrease in intrinsic volume (V_M) of the heme protein resulting from water penetration into the heme moiety and the substrate pocket is believed to be the reason for the pressure-induced high- to low-spin shift (*11*, *15*, *43*). In their study of pressure-induced transitions in P450cam, Fisher et al. (*42*) reported that saturating levels of camphor completely prevented the pressure-induced high-spin to low-spin transition at pressures below 800 bar. This observation convinced the authors that the pressure-induced spin transition is due solely to substrate dissociation from the enzyme. Notwithstanding this conclusion, the later studies have demonstrated that the pressure-induced spin-shift in P450cam takes place even at camphor saturation, but it requires pressures over 800 bar to be applied (*11*, *43*, *45*). However, a quantitative analysis of this transition is complicated by its overlapping with P450 conversion to P420, taking place in the same pressure range.

Studies of the effect of osmotic pressure on the interactions of P450cam with substrate (fenchone) and subsequent spin transitions of the heme protein (*15*) suggested that the volume changes in P450cam in these transitions could not be explained simply by changes in hydration of loosely bound water in the vicinity of the heme moiety. In these studies, 19 water molecules were implicated in the interactions of P450cam with fenchone and in the spin transition of the heme protein (*15*). The magnitude of this change is much higher than suggested from the degree of hydration of the substrate binding pocket near the heme moiety, where from six to nine crystallographically ordered water molecules were found in substrate-free P450cam (*10*). Thus, the interaction of P450cam with substrate and spin transitions of the heme protein were speculated to involve water bound at sites other than the substrate-binding site and the heme moiety (*15*). However, the technique employed in these studies with hydrostatic (*11*, *43*) and osmotic (*15*) pressure did not permit determination of whether solvent displacement was due to substrate binding or the subsequent low- to high-spin transition of the heme iron. Reaction volume changes derived from these experiments represent the overall values and include contributions from several elementary transitions, which may involve various types of waters of hydration (electrostricted, loosely bound in the protein cavities, etc.).

We have recently used the principal component analysis (PCA) technique for deconvolution of the spectra of P450 to resolve individual transitions in the heme protein (*44*, *46*). When used in high-pressure experiments, this permits the resolution of the reaction volume changes of the individual contributing processes, such as spin transitions and substrate binding (*44*). In our studies of rabbit liver microsomal P450 2B4 oligomers in solution (*44*) and in proteoliposomal membranes (*47*), we found that the pressure increase does not result in dissociation of the complex of P450 2B4 with benzphetamine. The effective volume changes on binding of benzphetamine to low-spin P450 2B4 were negligibly small. Instead, the low- to high-spin transition of the substrate complex was accompanied with an important positive volume change, which apparently indicates a dehydration of the protein (*44*, *47*). Another important conclusion from these studies is that P450 2B4 exhibits barotropic inhomogeneity in the oligomeric state. The two pressure-induced processes in P450 2B4, namely, the spin shift and conversion of P450 to P420, appear to occur in two different fractions of the heme protein. While approximately 65% of P450 2B4 molecules were always low-spin and could be converted from P450 to P420, the rest of the heme protein was not susceptible to pressure inactivation. Approximately 35% of the heme protein participated solely in the substrate- and pressure-dependent spin equilibria. This inhomogeneity of the heme protein apparently results from the organization of P450 oligomers, as it disappears on monomerization of

P450 2B4 by detergent (*44*). As eukaryotic cytochromes P450 are known to form oligomers not only in solution but also in membranes, this oligomerization-induced inhomogeneity of the heme protein may play an important role in the function and regulation of the monooxygenase. In the present paper, we describe pressure effects on the heme domain of P450BM3 (P450BMP), the bacterial heme protein which has the highest homology with microsomal P450s. In addition, the effect of hydrostatic pressure on cytochrome P450cam from *Pseudomonas putida* was reexamined at variable concentration of camphor. The barotropic parameters of substrate binding and spin transitions in P450BMP are compared with those obtained for P450cam and rabbit liver microsomal P450 2B4.

EXPERIMENTAL PROCEDURES

Materials. All chemicals were of ACS grade and were used without further purification. The purification of the heme protein domain of P450BM3 (P450BMP), from *E. coli* clones containing a plasmid encoding this protein, has been described previously (*48*). Purification of P450cam was done by a published procedure (*49*, *50*).

Experimental Spectral Measurements. The spectra were measured on a Cary-3 spectrophotometer (Varian, USA) in the 340−600 nm region with a 1 nm digitizing step. The computer-controlled optical pressure system, capable of generating a pressure of 7000 bar, has been described previously (*51*). After each adjustment of pressure, the system was allowed to stabilize for 3 min before measurement of the spectrum. At each pressure, at least 2 spectra were measured and averaged. All experiments with P450BMP were carried out at 25 °C in 100 mM Na−HEPES buffer, pH 7.4, containing 1 mM dithiothreitol and 1 mM EDTA. The experiments with P450cam were done in 100 mM Tris-HCl buffer (pH 7) containing 240 mM KCl at 4 °C.

Data Processing. To interpret the experiments in terms of pressure-induced changes in concentration of P450BMP species (high- and low-spin P450, and P420), a mathematical method based on principal component analysis (PCA) was used (*44*). This method is designed to resolve the optical changes in multicomponent systems into the separate components reflecting the concentration of each component in the system. It was also used to remove the spectral perturbations due to the changes in turbidity of the system during the experiments. Correction for turbidity was especially important in the presence of palmitic acid, which forms micelles whose size appears to be pressure-dependent. A minor component of the turbidity change was denaturation of some of the protein at high pressure. To interpret the pressure-induced transitions in terms of changes in concentration of P450 species, we used a least-squares fitting of PCA-decomposed spectra to the set of the spectral standards of high-spin, low-spin, and P420 forms of the heme protein (see "Results"). This approach was described in detail earlier (*44*, *46*).

Analysis of Pressure-Induced Transitions. The interpretation of pressure-induced changes is based on the equation for the pressure dependence of the equilibrium constant (*26*) (eq 1) where $K_{eq}(P)$ and K°_{eq} are the equilibrium constants of the reaction at pressure P and at zero pressure, respectively, $P_{1/2}$ is the pressure at which $K_{eq} = 1$ ("half-pressure" of the conversion), and ΔV° is the molar reaction volume. Control of the instruments, data acquisition, and fitting were done using our SPECTRALAB software package (*44*).

$$K_{eq}(P) = K^{\circ}_{eq} e^{-P\Delta V^{\circ}/RT} = e^{(P_{1/2}-P)\Delta V^{\circ}/RT} \qquad (1)$$

$$K^{\circ}_{eq} = e^{P_{1/2}\Delta V^{\circ}/RT}$$

RESULTS

Pressure-Induced Spectral Changes in P450BMP. A series of spectra of substrate-free P450BMP recorded as a function of increasing hydrostatic pressure is shown in Figure 1. In the initial stage (below 1.5 kbar), the difference spectra show a disappearance of the Soret band of high-spin P450BMP (λ_{max} = 396 nm) concomitant with an increase in absorbance at the position of the absorbance band of the low-spin heme protein (λ_{max} = 418 nm). This behavior was expected because a pressure-induced high- to low-spin shift of other P450s had been previously reported for P450cam (*15*, *45*), P450lin (*45*), and P450 2B4 (*44*, *47*). In the case of microsomal P450 2B4, the shift was observed even in the absence of substrate (*44*, *47*). A further increase in pressure results in the red shift of the P450BM3 Soret band from 418 to 425−426 nm. By analogy with that shown for P450cam (*45*) and P450 2B4 (*44*, *47*), this shift was attributed to the conversion of P450 to P420. These changes are complete at about 3500 bar. A further increase in pressure had no effect on the absorbance of P450BMP. When the system was decompressed from pressures below 1.5 kbar, where no conversion from P450 to P420 was observed, the changes (spin shift) were immediately and totally reversible. When the decompression was done from the higher pressures, the changes were also mostly reversible, but the conversion from P420 to P450 was slow. Depending on experimental conditions, the conversion required from 5 to 10 min to several hours (see below).

On completion of the process the maxima of the Soret band and α- and β-bands returned to the initial position, but the amplitude of the spectrum was in some cases considerably less than the initial level (Figure 1a, dotted line). Thus, the conversion of P450 to P420 caused by hydrostatic pressure was accompanied by some irreversible bleaching of the heme. This phenomenon had been observed earlier for P450 2B4 (*44*). While the bleaching of P450BMP was significant (20−30%) in the absence of substrate, addition of palmitic acid was shown to protect the protein. At saturating concentrations of palmitic acid (100 μM), no bleaching of the protein was observed and the pressure-induced changes appeared to be totally reversible.

For quantitative analysis of the pressure-induced changes, a set of standard spectra (high-spin, low-spin, and P420) is required. An attempt to use the set employed earlier for P450 2B4 (*44*, *46*) showed that the spectra of this mammalian heme protein do not fit the spectral changes in P450BMP. The most important difference was observed in the region of the Soret band of the spectra of the P420 heme proteins. To obtain the spectral standards of P450BMP, the procedure of backward fitting of the given spectra by the results of PCA of the experimental data was employed (*23*, *44*). A series of spectra measured at normal pressure at various concentrations of palmitic acid were used to obtain the

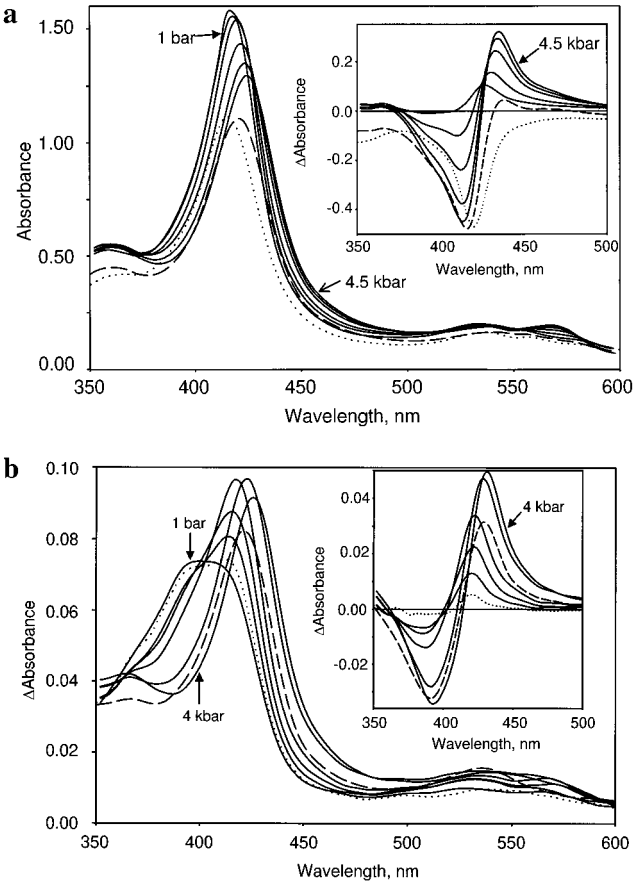

FIGURE 1: Pressure-induced changes in the absorbance spectra of P450BMP in the absence of fatty acid substrate. Conditions: 100 mM Na−Hepes buffer, pH 7.4, 1 mM EDTA, 1 mM dithiothreitol, 25 °C. The optical path length was 5 mm. (a, top): 30 μM P450BMP, no substrate present. Absolute spectra measured at 1, 1200, 2400, 3000, 3400, and 4500 bar, at 1 bar immediately after decompression from 5 kbar (dashed line), and 12 h after decompression (dotted line). The inset shows the results as the difference between the spectra at a particular pressure and the initial spectrum (at 1 bar). The difference between the spectra measured at normal pressure 12 h after decompression and prior to pressurization is shown by a dotted line. (b, bottom): 2.1 μM P450BMP, 8 μM palmitic acid. Absolute spectra were measured at 1, 800, 1200, 2000, 3200, and 4000 bar (solid lines), at 1 bar immediately after decompression from 5 kbar (dashed line), and at 20 min after decompression (dotted line). The inset shows the results as the difference between the spectra at a particular pressure and the initial spectrum at 1 bar (solid lines), the difference between the initial spectrum and the spectrum measured at normal pressure immediately after decompression is shown by a dashed line, and 30 min after decompression is shown by a dotted line.

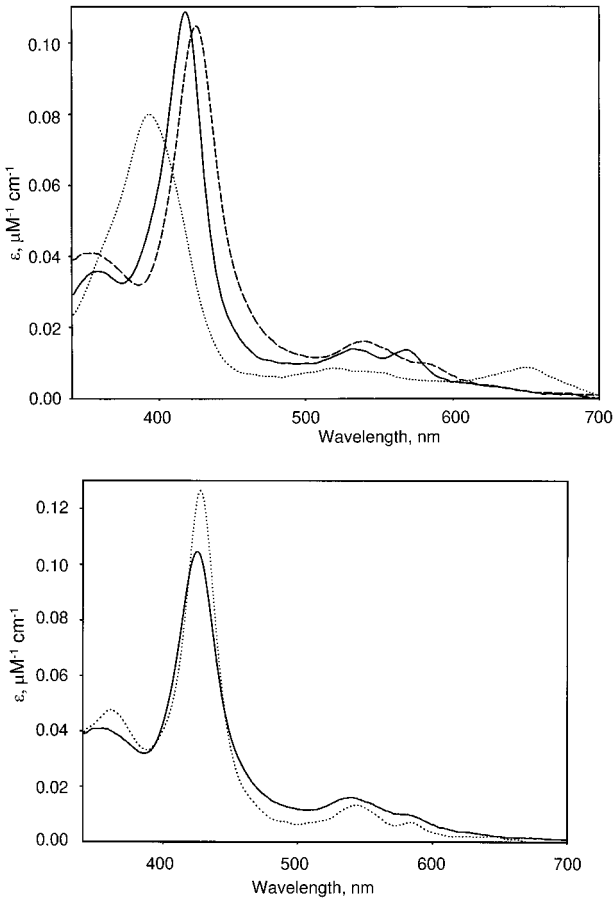

FIGURE 2: Standard spectra of pure high- and low-spin and P420 states of P450BMP deduced by PCA from the results of palmitic acid titration and pressure perturbation experiments. (a, top) Spectra of the low-spin (solid line), high-spin (dotted line), and P420 (dashed line) states of P450BMP; (b, bottom) spectra of P420BMP (solid line) and P450 2B4 (*46*).

standards of high- and low-spin states. To produce a spectrum of pure P420BMP, we used a series of spectra measured versus time at normal pressure during the conversion of P420 to P450 after a high-pressure experiment. The extinction coefficients for the high- and low-spin forms were verified by measurements of the total P450 concentration by the method of Omura and Sato (*52*). The extinction coefficient for P420 was evaluated from the requirement of conservation of the total heme protein concentration during recovery. The resulting spectra of the high- and low-spin forms of P450BMP are shown in Figure 2a. One can see that the spectra of P450BMP are similar to those of P450cam (*45*, *53*) and P450 2B4 (*44*, *46*). A minor difference between the spectra of P450BMP and P450 2B4 is observed in the structure of α- and β-bands of the low-spin heme proteins, which were found to be broader in the case of P450BMP. In contrast, there is a significant difference between P450BMP and P450 2B4 in the spectra of the P420 state (Figure 2b). Although the position of the maximum of the Soret band (425 nm) of P420BMP is close to that of P420 2B4 (427 nm) (*11*, *53*), the band is broader and the extinction coefficient at the maximum was only 105 mM^{-1} cm^{-1} compared with 128 mM^{-1} cm^{-1} for P420 2B4 (*46*). The α- and β-bands of P420BMP are also broader than those of P420 2B4. Despite these differences, the area under the spectrum in the 340−600 nm region remains unchanged.

Pressure-induced changes in the concentration of high-, low-spin, and P420 states of P450BMP in the absence of substrate and in the presence of 32 μM palmitic acid are shown in Figure 3. These results correspond to the above qualitative description. Exposure of P450BMP to high pressures induces a high- to low-spin, shift and a subsequent P450 to P420 transition, which is almost complete (more than 80% P420) at 4000 bar both in the presence and in absence of substrate. The whole pool of substrate-free P450BMP undergoes this transition in contrast to that shown for P450 2B4, where only about two thirds of the heme protein could be converted to the P420 state by high pressure (*44*, *47*, *54*).

To confirm the reliability of our spectral standards used in the treatment of the spectra of oxidized P420BMP, we

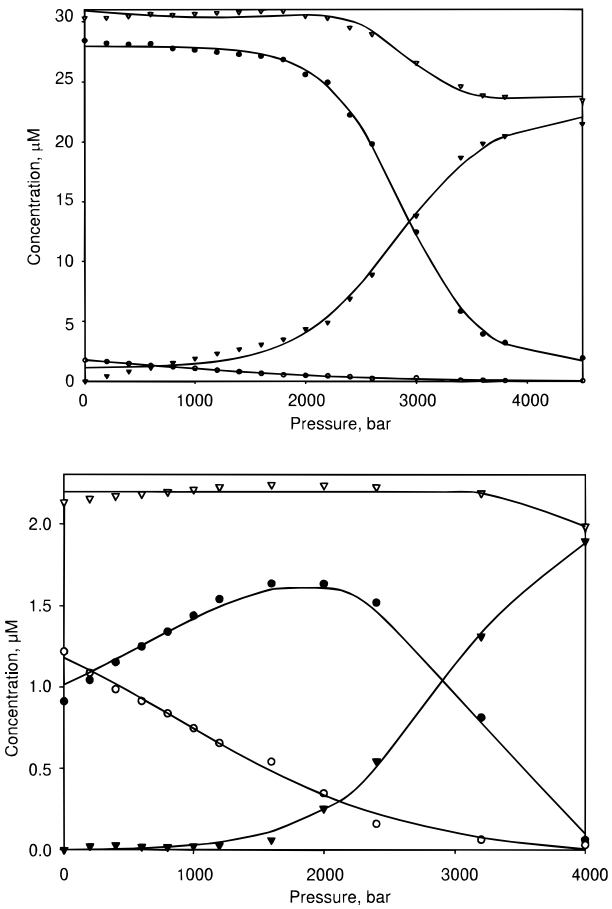

FIGURE 3: Pressure-induced changes in the concentrations of the high-spin (open circles), low-spin (filled circles), P420 (filled triangles), and the total heme protein (open triangles) in the absence of substrate (a, top) and in the presence of 8 μM palmitic acid (b, bottom). Other conditions were as those indicated for Figure 1.

have also determined the concentration of P420 and P450 forms of the heme protein during the process of conversion from the absorbance spectra of the reduced carbonyl complex of the heme protein mixture (*54*, *55*). This technique yields the same estimate of P420 content as derived from the spectra of oxidized heme protein. This agreement supports the identification of the pressure-induced red shift of the Soret band as the P450 to P420 transition of the heme protein. It also illustrates the applicability of the set of spectral standards for quantitative interpretation of the observed spectral changes. The calculation of the concentrations from the spectra of the reduced carbonyl complex also supports our conclusion regarding the reversibility of the P450-to-P420 conversion upon incubation after decompression. However, at the end of the process, when the spectra of the oxidized heme protein indicates no P420 present, the spectra of the reduced carbonyl complex still indicate that there is up to 40% of P420-like material in the samples. This suggests the presence of some form of P450BMP that has a Soret band of reduced carbonyl complex at 420 nm that is almost indistinguishable from the P450 state in the oxidized form. This result is in agreement with our observation of the multiplicity of P420 forms of P450BMP. A close examination of the spectra of P450BMP after recovery reveals a slight blue shift (1−2 nm) of the Soret maximum compared with the initial P450 state. Thus, the P420 state of P450BMP with P450-like spectral characteristics appears to have the Soret band blue-shifted compared to the position of the band of the "normal" P450 heme protein (418 nm).

Scheme 1

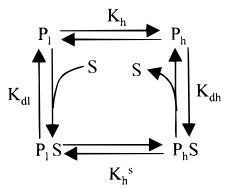

$$K_h = [P_h] / [P_l]\ ;\quad K_h^s = [P_hS] / [P_lS]\ ;$$
$$K_{dl} = [P_l][S] / [P_lS]\ ;\quad K_{dh} = [P_h][S] / [P_hS]$$

Scheme 2

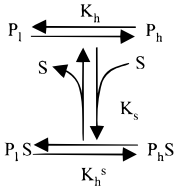

$$K_s = \frac{([P_l] + [P_h])\cdot[S]}{[P_lS] + [P_hS]}\ ;$$

$$K_s = \frac{(1 + K_h)\cdot K_{dl}}{1 + K_h^s} = \frac{(1 + K_h)\cdot K_{dl}\cdot K_{dh}}{K_{dh} + K_{dl}\cdot K_h}$$

Analysis of Substrate Binding and Spin Transitions of P450BMP. To perform an analysis of the pressure-induced changes in P450BMP substrate-binding and spin equilibria, we have used a four-state model of the transitions shown in Scheme 1, where "P" and "PS" correspond to P450 and its complex with the substrate, respectively. The subscripts "l" and "h" designate respectively the low- and high-spin states of the heme protein. To simplify the analysis, the two independent substrate binding equilibria of high- and low-spin P450 can be replaced by a single equilibrium characterized by an apparent dissociation constant, K_s (*56*), as shown in Scheme 2. These two schemes are formally equivalent, and the values of the parameters of the Scheme 2 can be used to calculate the parameters of the Scheme 1:

$$K_{dl} = \frac{K_s(1 + K_h^s)}{(1 + K_h)};\ K_{dh} = \frac{K_{dl}\cdot K_h}{K_h^s} \qquad (2)$$

To estimate the values of the equilibrium constants and the molar volume changes, a series of high-pressure experiments were performed at various concentrations of palmitic acid. The results were used to determine the dependence of the high-spin content of P450BMP as a function of pressure. These results were fit as a whole to the combination of the steady-state equilibrium equation corresponding to Scheme 2 with eq 1. The fitting gives the values of K_h^s, K_h, and K_s and the corresponding molar volume changes. The values of the constants K_{dl} and K_{dh} were then calculated using eq 2. In combination with the equation in Scheme 2, these relationships allow us to calculate K_{dl} and K_{dh} as a function of pressure. Then, the slopes of the plots of $\ln(K_{dl})$ and $\ln(K_{dh})$ versus pressure give the corresponding molar volume changes.

The experimental data and the fit to the proposed model shown in Figure 4 indicate that P450BMP behaves as a single entity that can undergo both spin equilibria and conversion from P450 to P420. This is in contrast to P450 2B4 in

Table 1: Equilibrium Constants and Reaction Volumes of Substrate Binding and Spin Transitions of P450BMP (with Palmitic Acid as Substrate), P450cam (with Camphor as Substrate), and P450 2B4[a] (with Benzphetamine as Substrate)[a,b]

	equilib const at zero pressure			$\Delta V°$,[d] mL/mol		
transition[c]	BMP	P450cam	2B4	BMP	P450cam	2B4
$P_l \leftrightarrow P_h$ (K_h)	0.19	0.013	0.32	23	20	21
$P_lS \leftrightarrow P_hS$ (K_hs)	1.2	62	8.3	16	91	49
$PS \leftrightarrow P + S$ (K_s)	2.1 μM	4.4 μM	130 μM	−25	−48	8.1
$P_lS \leftrightarrow P_l + S$ (K_{dl})	3.9 μM	280 μM	930 μM	−20	42	5.3
$P_hS \leftrightarrow P_h + S$ (K_{dh})	0.61 μM	0.047 μM	36 μM	−13	−29	−23

[a] The values given for P450 2B4 are from our previous publication (*44*). The original paper contains only the values for the transition calculated for the simplified model (Scheme 2). The values of K_{dl} and K_{dh} (lower portion of the table) were calculated from the original values as described in the text. [b] The values given for P450 2B4 and P450BMP were determined at 25 °C, while those of P450cam were measured at 4 °C. The estimates of the equilibrium constants and reaction volumes given in this table are characterized by standard deviations of no more than 12% of their values, except for the estimates of K_{dl} and K_{dh} and corresponding reaction volumes (lower portion of the table) whose standard deviations are higher (20−40% of the values). [c] The designations used here correspond to those used for Schemes 1 and 2. [d] The sign of the reaction volume corresponds to the low- to high-spin and substrate complex dissociation reactions.

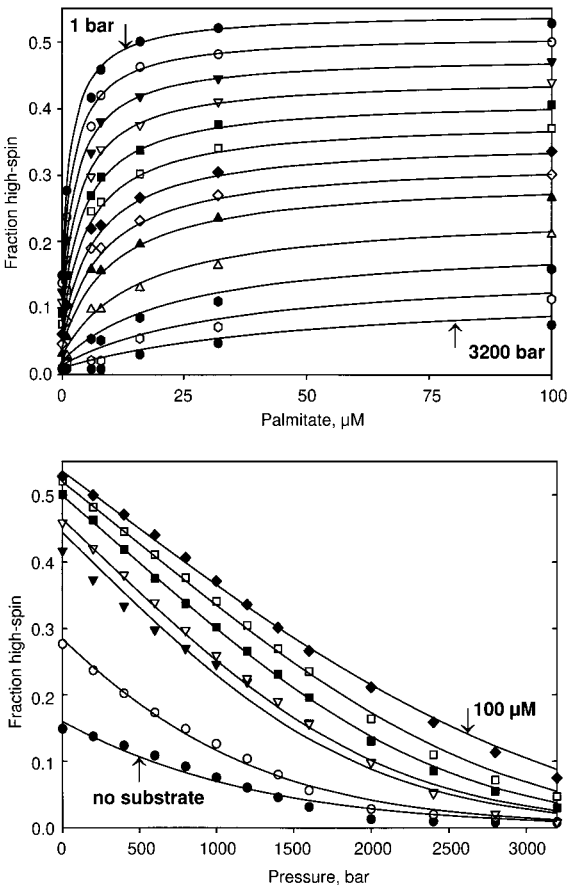

FIGURE 4: Effect of pressure on the high-spin content in P450BMP as a function of the concentration of palmitic acid. The same data set is shown as follows: (a, top) a series of the palmitic acid−titration curves measured at 1, 200, 400, 600, 800, 1000, 1200, 1400, 1600, 2000, 2400, 2800 and 3200 bar; (b, bottom) a series of the pressure dependencies measured in the absence of substrate and at 1, 6, 8, 16, 32, and 100 μM palmitic acid. Solid lines show the results of the fitting of this data set to the equation for the pressure dependence of the system in Scheme 1 with the parameters shown in Table 1.

solution where the fraction undergoing the P450 to P420 transition was found to exclude the fraction that underwent the substrate-dependent spin transition (*44*, *47*).

The values of the constants of the elementary transitions and the corresponding $\Delta V°$ values are compared with those found for P450 2B4 (*44*) in Table 1. The conversion of both substrate-free and substrate-bound P450BMP from the high- to low-spin state is accompanied by a volume decrease (−23 and −16 mL/mol, respectively). Dissociation of the substrate complex of both low- and high-spin P450BMP is also characterized by a negative volume change (−20 and −13 mL/mol correspondingly).

Analysis of the P450 to P420 Transition of P450BMP. The pressure dependence of the P420 content in P450BMP at several concentrations of palmitic acid is shown in Figure 5a. The parameters of the pressure-induced P450 to P420 transition of P450BMP exhibits clear dependence on the concentration of substrate. In the case of P450BMP, the molar volume change for the conversion of P450 to P420 in the absence of substrate was −99 mL/mol. This value is decreased to −42 mL/mol by the addition of palmitic acid (32 μM). The decrease in the reaction volume is accompanied by an increase in the $P_{1/2}$ value from 2.1 kbar in the absence of substrate to 3.1 kbar with 32 μM palmitic acid. However, since pressure induces a dissociation of the substrate complex of P450BMP (see above), these $\Delta V°$ and $P_{1/2}$ values for the P450 to P420 transition in the presence of substrate should be considered as "apparent". The pressure dependence of the P420 content in P450BMP in the presence of substrate should not fit eq 1 precisely, since the reaction is composed of at least two distinct pressure-dependent processes (dissociation of the substrate complex and the P450 to P420 transition of substrate-free enzyme). If dissociation of the substrate complex of P450BMP is required for conversion of P450BMP into P420, the behavior of the system can be predicted from the values shown in Table 1 and the parameters of the P450 to P420 transition of substrate-free heme protein ($\Delta V° = -99$ mL/mol, $P_{1/2} = 2.1$ kbar). Although the modeling curves built in this way (Figure 5b) do not fit the experimental data precisely, the qualitative behavior of the model is very similar to that observed in the experiment (Figure 5). Thus, the above hypothesis can be taken as a rough estimate of reality. For example, fitting of the modeling curve for 32 μM palmitic acid by the equation in Scheme 1 gives values of $\Delta V°$ and $P_{1/2}$ of −47 mL/mol and 2.7 kbar, which are close to experimentally determined values (−42 mL/mol and 3.1 kbar, respectively). Thus, an apparent decrease in $\Delta V°$ for the P450 to P420 transition in the presence of substrate is explainable by the fact that in the latter case the inactivation is preceded by pressure-induced dissociation of the P450BMP-substrate complex.

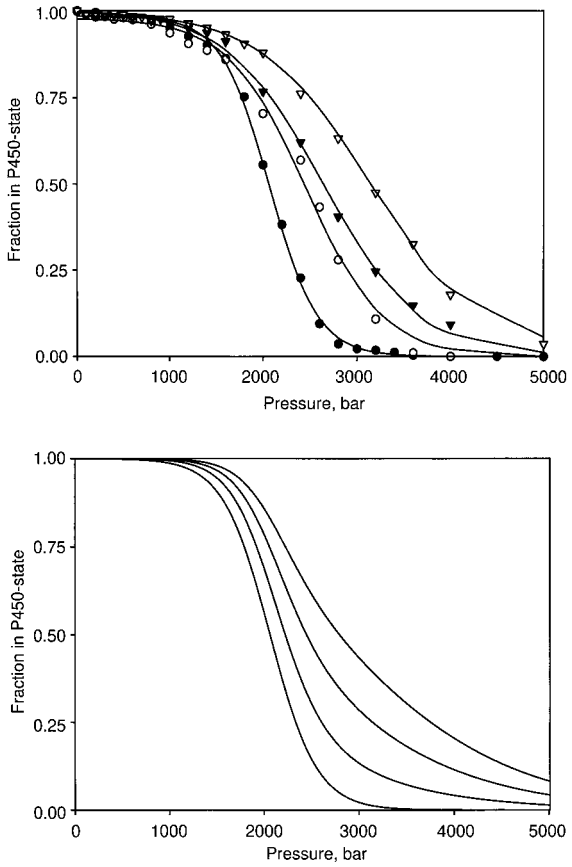

FIGURE 5: Pressure-induced conversion of P450BMP into P420. (a, top) The dependencies of the P420 content on pressure are shown at no substrate present (closed circles) and at 6 (open circles), 16 (closed triangles), and 32 μM (open triangles) palmitic acid. Solid lines show the results of the fitting of these data to the equation of pressure dependence of the equilibrium of a single transition (eq 1). (b, bottom) Modeling of the pressure-induced P450 to P420 transition in P450BMP by the combination of the equilibrium system of Scheme 1 with a single reversible P450-to-P20 transition of the substrate-free heme protein (i.e. from the assumption, that the substrate-bound P450BMP does not undergo the inactivation). The experimentally obtained parameters for the substrate binding, spin transitions (Table 1), and P450-to-P420 conversion of the substrate-free P450BMP ($\Delta V^\circ = -99$ mL/mol, $P_{1/2} = 2.1$ kbar) were used in the modeling. The curves were calculated for 0, 6, 16, and 32 μM palmitic acid.

As described above, the pressure-induced conversion of P450BMP to P420 is partially reversible. The kinetics of the P420 conversion to P450 after decompression are shown in Figure 6 at two different concentrations of P450BMP. The kinetics show a clear dependence on P450BMP concentration. At 8.5 μM P450BMP the recovery took about 12 h, while at 0.5 μM P450BMP there was an almost complete recovery in a few minutes after decompression from 5 kbar. To explain this dependence, we assume that P420BMP forms aggregates with a K_d in the range of 0.5 and 7 μM and that aggregation stabilizes P420 and prevents it from recovery to P450.

Analysis of Substrate Binding and Spin Transitions in P450cam. As it was stated above, despite extensive studies of pressure-induced transitions in P450cam, the barotropic parameters of the individual transitions of the four-step equilibrium model (Scheme 1) had not been determined. All previous experiments were done in the absence or at saturating concentrations of substrates, which did not permit

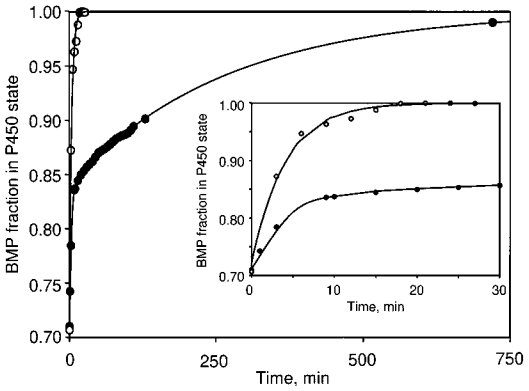

FIGURE 6: Kinetics of the conversion of pressure generated P420BMP back to the P450 state after decompression. Curves were recorded at 0.5 (open circles) and 8.5 μM (filled circles) P450BMP. The inset shows the initial portions of the same curves. Solid lines represent the results of data fitting. The curve measured at 0.5 μM P450BMP obeys a single-exponential equation with a kinetic constant of 0.26 min^{-1}. The curve for 8.5 μM P450BMP was fit to the equation of the sum of two exponents with kinetic constants of 0.27 min^{-1} and 0.23 h^{-1} and the 45% fraction of the fast phase.

us to resolve the volume changes in the spin transition from those of dissociation of the substrate complex. To fill that gap, we have studied pressure-induced transitions in P450cam as a function of the concentration of camphor. The pressure-induced spectral changes of P450cam are very well documented, and our results are completely consistent with previous observations (*11*, *27*, *43*). Similar to that reported here for P450BMP, an increase in hydrostatic pressure results in a high- to low-spin transition of P450cam followed by the pressure-induced formation of the P420 state of the heme protein. In agreement with earlier data for P450cam (*11*, *27*) and in contrast to that observed here for P450BMP, the pressure-induced inactivation of P450cam was almost irreversible. To simplify the interpretation of the results and to improve the resolution of the pressure-induced spin transitions from the inactivation of the heme protein, all experiments with P450cam were carried out at 4 °C. At this temperature the overlapping of pressure-induced spin shift and inactivation was minimal. In agreement with previous observations, pressure-induced inactivation of P450cam was accompanied by prominent bleaching of the Soret band concomitant with the appearance of spectral bands near 365 and 454 nm (*11*, *27*). To increase the accuracy of the determination of the spin state in our experiments with P450cam, the weighting coefficients for the spectral regions of these bands (355−375 and 435−465 nm) were set to minimum when fitting the data by the spectral standards of P450ls, P450hs, and P420 states.

The series of pressure dependencies of the spin state of P450cam measured at various concentrations of camphor is shown in Figure 7. As can be seen in that figure, our results fit the four-equilibrium model (Scheme 1). The values of the barotropic parameters derived from this fitting are shown in Table 1.

DISCUSSION

Despite the differences in the gene and protein sequences of members of the P450 gene superfamily, the structures of the five that are published (*57*−*60*) are remarkably similar in the structural core. Although the structure of the heme

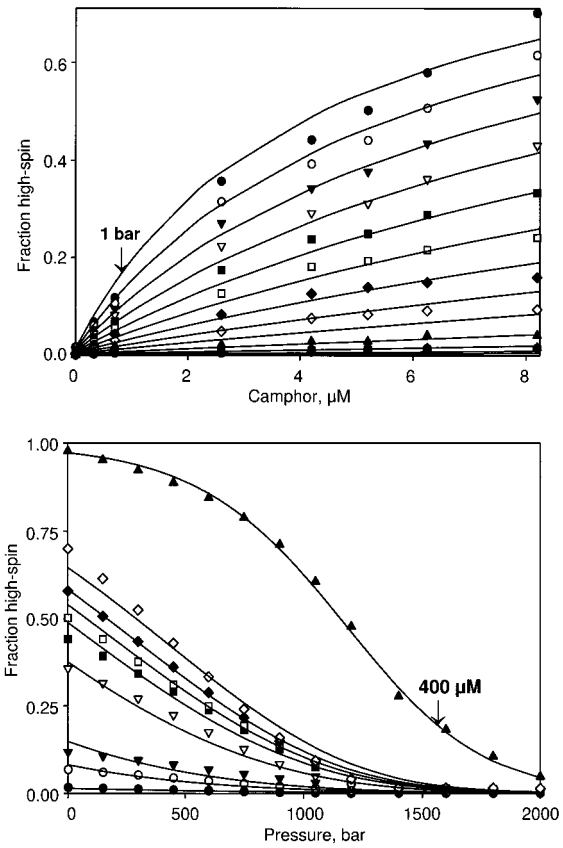

FIGURE 7: Effect of pressure on the high-spin content in P450cam as a function of the concentration of camphor. Conditions: 3 μM P50cam in 100 mM Tris-HCl, pH 7.4, 240 mM KCl; 4 °C. The same data set is shown as follows: (a, top) as a series of the camphor−titration curves measured at 1, 150, 300, 450, 600, 750, 900, 1050, 1200, 1400, 1600, 1800, and 2000 bar; (b, bottom) a series of the pressure dependencies measured in the absence of substrate and at 0.33, 0.7, 2.6, 4.2, 5.2, 6.25, 8.2, and 400 μM camphor; solid lines show the results of the fitting of this data set by the equation for the pressure dependence of the system illustrated by the Scheme 1 with the parameters shown in Table 1.

moiety of the cytochromes P450 is well-characterized, the nature of the P420 form of these enzymes is almost unknown. The process of conversion of "P450" to "P420" is poorly understood, and no unifying concepts are currently available to account for this conversion. The pressure-induced transition of P450BMP into the P420 state and P450 2B4 into its P420 state is distinctly different for these heme proteins. In the oligomers of P450 2B4, the maximal ratio of the conversion to P420 is never higher than 65−70% due to the presence of two independent populations of the heme protein that undergo substrate- and pressure-dependent equilibria (*44*). In contrast, soluble monomeric bacterial P450cam and P450BMP behave as single entities undergoing both spin equilibria and the P450 to P420 transition (*44*, *47*). Our present data on P450cam and P450BMP support the prior conclusion that the apparent heterogeneity of P450 2B4 in its barotropic behavior is due to the oligomeric nature of this membrane-bound protein.

The very high $\Delta V°$ for the P450 to P420 conversion of P450BMP suggests some important hydration of the protein accompanies this transition. This hydration is difficult to explain only by the water flux into the heme moiety. A $\Delta V°$ this large can only result from an increase of the water-accessible surface of the protein. The broad absorbance bands both in the Soret and visible regions of the spectrum of P420BMP suggest some multiplicity of this state and apparently reflects a very flexible conformation of this P420 heme protein. The dependence of the kinetics of the backward conversion of P420 to P450 on the initial concentration of P450BMP indicates that the P420 form of P450BMP tends to aggregate and this aggregation stabilizes the enzyme in the P420 state. This conclusion also suggests that the transition between P450 and P420 states of P450BMP requires a rearrangement of the protein involving surface-exposed regions. These surface-exposed residues create P420−P420 interaction sites, promote aggregation, and appear to stabilize the heme protein in the P420 state. The results presented here and our previous results make studies of the effects of pressure-induced transitions on the secondary structure of P450 heme proteins important for understanding the nature of the P420 state and the mechanisms of aggregation.

Our prior studies of pressure effects did not include a detailed analysis of the volume changes for substrate binding and the spin transitions of P450 2B4 due in part to the fact that only the values for the transitions in the simplified three-equilibrium model (Scheme 2) were determined. In the present paper, we have described a simple way to deduce the volume changes for the four-state equilibrium model (Scheme 1). Also, in the present study we have for the first time resolved the volume changes in P450cam into the values for each step of the four-state equilibrium model. The newly obtained values of volume changes in substrate binding and spin-state transition in all three P450s are presented in Table 1. If the values of $\Delta V°$ for spin-state transitions allow direct comparison, the analysis of the values of $\Delta V°$ for substrate dissociation requires the differences in the partial volumes of the substrates to be taken into account.

Dissociation of the substrate complex of P450cam was assumed to be accompanied by a negative volume change because of water penetration into the vicinity of the heme moiety and the substrate pocket. Despite these expectations, our analysis shows that the volume change in the dissociation of the low-spin form of the camphor-bound heme protein is positive. Therefore, an increase in hydrostatic pressure induces formation of the substrate complex and, simultaneously, shifts the spin state of the camphor-bound P450cam toward the low-spin form. These results are in contrast with the previous conclusion of Fisher et al. (*42*) that the pressure-induced spin shift in P450cam reflects the pressure-induced dissociation of the substrate complex. This conclusion was based on the observation that hydrostatic pressure has almost no effect on the spin state of the substrate-saturated enzyme. However, as can be seen in Figure 7, the pressure region (1−800 bar) used in this analysis is not enough to probe pressure-induced spin transitions. Our analysis clearly shows that the conclusion of Fisher et al. is incorrect and the pressure-induced spin shift in P450 is due to the displacement of the spin equilibrium of the substrate-bound enzyme and not to the dissociation of the complex.

The volume changes measured by pressure perturbation represent a bulk effect over the whole system; therefore, the volume decrease due to removal of the substrate molecule from solution must also be considered. The volume changes upon the interactions of the heme protein with the substrate are composed of the changes in the partial volume of the

protein as well as the volume change due to incorporation of the substrate molecule into the substrate pocket. Thus, the interpretation of the values of $\Delta V°_{diss}$ requires the partial volume ($V°$) of the substrate to be taken into account.

The values of $V°$ for small organic solutes can be estimated using a semiempiric equation proposed by Kharakoz (*30*). This equation was implemented here in the following form:

$$V° = V_M + a_S S_M + b_S + V_I + \beta_{T0} RT \qquad (3)$$

This equation was obtained by substitution of the thermal volume V_T term by its empirical approximation, $V_T = a_S S_M + b_S$, where S_M is the surface of the molecule. The values of a_S and b_S were estimated to be 0.249 mL/(mol·Å^2) and 4 mL/mol correspondingly, if the "van der Waals" volume and surface values are used for V_M and S_M (*30*). The interaction volume V_I might be estimated as a sum of the contributions of −6 mL/mol per each polar atom in the molecule (*30*). The "ideal term", $\beta_{T0}RT$, was taken as 1 mL/mol (*30*, *31*). To calculate the van der Waals volume and surface we used the "SPACEFILL" utility from "TINKER" molecular mechanics software toolkit (*61*), which is available from Prof. J. W. Ponder at http://dasher.wustl.edu/tinker.

Using the method above (*62*), the partial volume of camphor in water solution was calculated to be about 148 mL/mol. Therefore, the volume changes due to incorporation of camphor into the substrate pocket could account for approximately −148 mL/mol. However, the experimental value of the reaction volume of complex formation (the negative of $\Delta V°$ for substrate binding given in Table 1) was determined to be −42.2 mL/mol. Therefore, the changes in partial volume of the protein on camphor binding may be determined as the difference between this value and the partial volume of camphor giving an estimate of +106 mL/mol.

It is assumed that as the compressibility of the protein core is rather small and the intrinsic volume ("van der Waals volume") of the protein core can be considered constant, the changes in the protein partial volume reflect primarily the changes in the protein hydration (*28*, *29*). At first glance, we can consider the changes in $V°$ as the bulk effect of the hydration/dehydration of the protein cavities (V_M term) and the changes in the water density around the protein molecule due to the exposition of its hydrophobic and polar regions to the water phase (V_T and V_I terms). Due to the complex nature of the $\Delta V°$ values, they cannot be used to make any definitive conclusion on the hydration changes. However, for the qualitative analysis we can apply an oversimplified suggestion that all changes in the partial volume of the protein are due to the hydration/dehydration of the protein cavities. Assuming the volume change due to the penetration of one water molecule into the protein cavity of 18.1 mL/mol, which is the partial volume of water in the bulk solvent (*37*, *38*), one can estimate the minimal number of waters implicated in the transition. The estimates obtained in this way should be considered as a very coarse approximation of the minimal number of water molecules employed in the changes of the protein hydration. This approach can be used to judge whether the observed volume changes are explainable only by water penetration into the active site of P450, or we can assume some other regions of the protein to be involved in the hydration changes. If we assume that the above calculated volume change of +106 mL/mol ise due solely to dehydration of the heme moiety and the substrate pocket, we should expect that formation of the substrate complex of low-spin P450cam requires expulsion of at least six water molecules from the protein.

A subsequent transition of the low-spin P450cam complex with camphor into the high-spin form is characterized by a volume change of 90.6 mL/mol (Table 1). The sum of this value with the above estimate of +106 mL/mol gives a value of about 197 mL/mol for the total volume change in the transition of low-spin substrate-free P450cam into the high-spin camphor-bound form. If the reported change in the partial volume of P450cam results solely from the hydration of empty cavities in the molecule of protein, then this transition has to be accompanied by expulsion of at least 11 water molecules. This number is almost two times lower than the estimate of 19 molecules derived from osmotic stress studies (*15*). Our estimate is not too far from the maximal changes in the hydration of the active site of P450cam from theoretical considerations. Examination of the X-ray structure shows that substrate-free P450cam contains six crystallographically ordered water molecules in the immediate vicinity of the heme moiety (*10*). Molecular mechanics calculations show the possible locations for up to three additional water molecules in the active site of P450cam (*12*). It is suggested, that two to three water molecules displaced from the active site by substrate binding occupy the substrate-access channel; the rest of the displaced water molecules have to be excluded to bulk solvent (*11*, *15*, *43*). Therefore, the total changes in the active site hydration on the substrate binding and spin shift in P450cam are expected to be in the range of 3−7 water molecules (54−137 mL/mol), which is not dramatically lower than the estimate of 197 mL/mol derived from the present study. Thus, the changes in the partial volume of P450cam on camphor binding and spin transition are explainable from the suggestion that they are due solely to the changes in the hydration of the active site of P450. However, we cannot completely exclude the possibility that the formation of the complex of P450cam with substrates also involves dehydration of some loci outside of the active site of the heme protein (*15*).

The $\Delta V°$ for dissociation of the benzphetamine complex of low-spin P450 2B4 is positive and differs from the value found for P450cam by 37 mL/mol (Table 1). The volume change on dissociation of the low-spin P450BMP−palmitic acid complex is negative, and its difference from the value found for the P450cam complex with camphor is 62.3 mL/mol. It should be noted that camphor is the smallest of the three substrates. Calculation of the partial volumes for benzphetamine and palmitic acid using eq 3 (*62*) as described above yields volumes of 263 and 268 mL/mol, respectively. Taking into account these volumes and using the values of $\Delta V°$ for dissociation of the substrate complexes presented in Table 1, we estimated the changes in the partial volume of the proteins on their interactions with substrates to be about 267 mL/mol for the P450 2B4−benzphetamine pair and 248 mL/mol for P450BMP interactions with palmitic acid. These changes are considerably larger than the value of 106 mL/mol calculated above for the interactions of P450cam with camphor. In contrast with P450cam, the volume changes in 2B4 and BMP are too large to be accounted for solely by changes in hydration of the active

site. These results suggest that the interactions of P450BMP and P450 2B4 with their substrates induce important dehydration of sites other than the heme moiety and the substrate pocket. Thus, structural rearrangements in both P450 2B4 and P450BMP on substrate binding appear to be more profound than in the case of P450cam. This conclusion is in agreement with the data on the high flexibility of P450BMP (*63*) and important structural rearrangements in this heme protein caused by interactions with the substrates (*64*−*66*). This comparison also suggests that the mechanism of substrate-induced transitions in P450 2B4 is more similar to those in P450BMP than in P450cam.

All three heme proteins have similar values for $\Delta V°$ of the spin transition of the substrate-free enzyme (20−23 mL/mol). This volume change is consistent with expulsion of one water molecule (18.1 mL/mol) from the protein. This result appears to be reasonable in view of the fact that the transition of low- to high-spin P450 is accompanied by dissociation of the sixth water ligand from the heme iron (*7*). Expulsion of this water ligand from the heme moiety of P450BMP was recently shown by NMR experiments (*65*).

While all three heme proteins show similar values of $\Delta V°$ for the spin-state transition in the substrate-free state, there are important differences in this value when determined for their complexes with substrates. Both substrate-free and substrate-bound P450BMP shows similar values of $\Delta V°$ for the spin-state transition (16−23 mL/mol), and this volume is consistent with a release of one water molecule from the substrate pocket. However, in the case of P450cam, binding of camphor results in an increase of $\Delta V°$ for the spin-state transition from 20 to 91 mL/mol. It suggests that the transition of the camphor-bound heme protein into the low-spin state requires significant hydration of the protein when compared to the substrate-free enzyme. This difference of 71 mL/mol is consistent with additional occupancy of four water molecules in the heme moiety of the substrate-free high-spin P450cam compared with the high-spin form of the camphor-bound heme protein. The complex of P450 2B4 with benzphetamine has an intermediate position between P450cam−camphor and P450BMP−palmitic acid complexes by the value of $\Delta V°$ for the spin-state transition.

In a recent study of the interactions of P450cam with a series of analogues of camphor, a linear relationship between $\Delta V°$ and $\Delta G°$ for the spin-state transition was demonstrated (*67*). In these experiments, the concentration of camphor and its analogues was kept at 400 μM, in the presence of 240 mM KCl, and the spectral changes below 1500 bar were used to determine $\Delta V°$ values for the spin-state transition (*67*). Using the data presented in Table 1, we can calculate that in these experiments the degree of saturation of P450cam with substrates was always higher than 80% and pressure-induced changes in the concentration of the substrate-bound heme protein could be neglected. Therefore, the effective values of $\Delta V°$ for the spin-state transition determined by Helms et al. (*67*) may be interpreted as volume changes in the spin transition of the substrate-bound P450cam. Comparing our results with their data (*67*), we have found that the whole series of $\Delta V°/\Delta G°$ data pairs for the spin-state transition obey the same linear dependence. The points obtained in both studies fall around the same straight line (Figure 8). Therefore, the linear relationship between $\Delta V°$ and $\Delta G°$ for the spin-state transition appears to be a general feature of P450 heme proteins and suggests a common mechanism of the shift of spin equilibrium by substrate binding for the three heme proteins studied here. The transition of the substrate-bound P450 from the high- to low-spin state (without release of the substrate) requires more hydration than in the case of the substrate-free heme protein, where only one water molecule apparently enters the heme moiety on this transition. $\Delta G°$ of the spin shift may be thought of as linearly connected with the number of water molecules required to enter the heme moiety for the transition of the substrate-bound heme protein into the low-spin form. This finding may be important in understanding the mechanism of interaction of cytochromes P450 with their substrates and the substrate-induced spin shift.

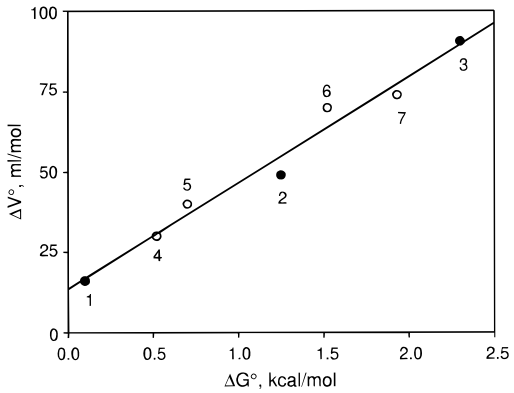

FIGURE 8: Correlation between molar volume change ($\Delta V°$) and the change in Gibbs free energy ($\Delta G°$) in the low to high-spin transition of substrate-bound cytochromes P450. Filled circles represent the results obtained in the present study for P450BMP/palmitic acid (1), P450 2B4/benzphetamine (2), and P450cam/camphor (3) pairs. Data shown in open circles are taken from the work of Helms and coauthors (*67*) and represent the results obtained for the complexes of P450cam with *endo*-borneol *O*-methyl ether of camphor (4), *endo*-borneol *O*-propyl ether of camphor (5), *endo*-borneol *O*-allyl ether of camphor (6), and camphor (7).

REFERENCES

1. Parsegian, V. A., and Rau, D. C. (1984) *J. Cell Biol. 99*, 196s−200s.
2. Rupley, J. A., and Careri, G. (1991) *Adv. Protein Chem. 41*, 37−172.
3. Schoenborn, B. P., Garcia, A., and Knott, R. (1995) *Prog. Biophys. Mol. Biol. 64*, 105−119.
4. Reid, C., and Rand, R. P. (1997) *Biophys. J. 72*, 1022−1030.
5. Covell, D. G., and Wallqvist, A. (1997) *J. Mol. Biol. 269*, 281−297.
6. Poornima, C. S., and Dean, P. M. (1995) *J. Comput.-Aided. Mol. Des. 9*, 500−512.
7. Griffin, B. W., and Peterson, J. A. (1975) *J. Biol. Chem. 250*, 6445−6451.
8. Philson, S. B., Debrunner, P. G., Schmidt, P. G., and Gunsalus, I. C. (1979) *J. Biol. Chem. 254*, 10173−10179.
9. Poulos, T. L., Finzel, B. C., and Howard, A. J. (1986) *Biochemistry 25*, 5314−5322.
10. Poulos, T. L., Finzel, B. C., and Howard, A. J. (1987) *J. Mol. Biol. 195*, 687−700.
11. Hui Bon Hoa, G., Di Primo, C., Geze, M., Douzou, P., Kornblatt, J. A., and Sligar, S. G. (1990) *Biochemistry 29*, 6810−6815.
12. Wade, R. C. (1990) *J. Comput.-Aided. Mol. Des. 4*, 199−204.
13. Di Primo, C., Sligar, S. G., Hui Bon Hoa, G., and Douzou, P. (1992) *FEBS Lett. 312*, 252−254.
14. Loida, P. J., and Sligar, S. G. (1993) *Biochemistry 32*, 11530−11538.

15. Di Primo, C., Deprez, E., Hui Bon Hoa, G., and Douzou, P. (1995) *Biophys. J. 68*, 2056−2061.
16. Helms, V., and Wade, R. C. (1995) *Biophys. J. 69*, 810−824.
17. Oprea, T. I., Hummer, G., and Garcia, A. E. (1997) *Proc. Natl. Acad. Sci. U.S.A. 94*, 2133−2138.
18. Ravichandran, K. G., Boddupalli, S. S., Hasemann, C. A., Peterson, J. A., and Deisenhofer, J. (1993) *Science 261*, 731−736.
19. Deprez, E., Gerber, N. C., Di Primo, C., Douzou, P., Sligar, S. G., and Hui Bon Hoa, G. (1994) *Biochemistry 33*, 14464−14468.
20. Gerber, N. C., and Sligar, S. G. (1994) *J. Biol. Chem. 269*, 4260−4266.
21. Benson, D. E., Suslick, K. S., and Sligar, S. G. (1997) *Biochemistry 36*, 5104−5107.
22. Di Primo, C., Deprez, E., Sligar, S. G., and Hui Bon Hoa, G. (1997) *Biochemistry 36*, 112−118.
23. Zhukov, A. A., and Archakov, A. I. (1985) *Biokhimiia 50*, 1939−1952.
24. Kornblatt, J. A., and Hui Bon Hoa, G. (1990) *Biochemistry 29*, 9370−9376.
25. Cioni, P., and Strambini, G. B. (1997) *Biochemistry 36*, 8586−8593.
26. Weber, G. (1991) in *Protein Interactions*, Chapman and Hall, New York.
27. Hui Bon Hoa, G., Di Primo, C., and Douzou, P. (1992) in *High Pressure and Biotechnology* (Balny, C., Hayashi, R., Heremans, K., and Masson, P., Eds.) pp 139−145, Libby Eruotext Ltd., Montrouge, France.
28. Masson, P., and Balny, C. (1988) *Biochim. Biophys. Acta 954*, 208−215.
29. Kharakoz, D. P. (1997) *Biochemistry 36*, 10276−10285.
30. Kharakoz, D. P. (1989) *Biophys. Chem. 34*, 115−125.
31. Chalikian, T. V., and Bresiauer, K. J. (1996) *Biopolymers 39*, 619−626.
32. Gerstein, M., Tsai, J., and Levitt, M. (1995) *J. Mol. Biol. 249*, 955−966.
33. Burling, F. T., Weis, W. I., Flaherty, K. M., and Brunger, A. T. (1996) *Science 271*, 72−77.
34. Gerstein, M., and Chothia, C. (1996) *Proc. Natl. Acad. Sci. U.S.A. 93*, 10167−10172.
35. Chalikian, T. V., and Breslauer, K. J. (1996) *Proc. Natl. Acad. Sci. U.S.A. 93*, 1012−1014.
36. Stranks, D. R. (1974) *Pure Appl. Chem. 38*, 303−323.
37. Millero, F. J. (1972) in *Water and Aqueous Solutions* (Horn, R. A., Ed.) pp 519−595, Wiley-Interscience, New York.
38. Colombo, M. F., Rau, D. C., and Parsegian, V. A. (1992) *Science 256*, 655−659.
39. Hubbard, S. J., Gross, K. H., and Argos, P. (1994) *Protein Eng. 7*, 613−626.
40. Hubbard, S. J., and Argos, P. (1994) *Protein Sci. 3*, 2194−2206.
41. LaLonde, J. M., Bernlohr, D. A., and Banaszak, L. J. (1994) *Biochemistry 33*, 4885−4895.
42. Fisher, M. T., Scarlata, S. F., and Sligar, S. G. (1985) *Arch. Biochem. Biophys. 240*, 456−463.
43. Di Primo, C., Hui Bon Hoa, G., Douzou, P., and Sligar, S. G. (1992) *Eur. J. Biochem. 209*, 583−588.
44. Davydov, D. R., Deprez, E., Hui Bon Hoa, G., Knyushko, T. V., Kuznetsova, G. P., Koen, Y. M., and Archakov, A. I. (1995) *Arch. Biochem. Biophys. 320*, 330−344.
45. Hui Bon Hoa, G., Di Primo, C., Dondaine, I., Sligar, S. G., Gunsalus, I. C., and Douzou, P. (1989) *Biochemistry 28*, 651−656.
46. Renaud, J. P., Davydov, D. R., Heirwegh, K. P., Mansuy, D., and Hui Bon Hoa, G. (1996) *Biochem. J. 319*, 675−681.
47. Davydov, D. R., and Hui Bon Hoa, G. (1997) in *High-Pressure Research in the Biosciences and Biotechnology* (Heremans, K., Ed.) pp 111−114, Leuven University Press, Leuven, Belgium.
48. Boddupalli, S. S., Oster, T., Estabrook, R. W., and Peterson, J. A. (1992) *J. Biol. Chem. 267*, 10375−10380.
49. Gunsalus, I. C., and Wagner, G. C. (1978) *Methods Enzymol. 52*, 166−188.
50. Atkins, W. M., and Sligar, S. G. (1988) *J. Biol. Chem. 263*, 18842−18849.
51. Hui Bon Hoa, G., and Marden, M. C. (1982) *Eur. J. Biochem. 124*, 311−315.
52. Omura, T., and Sato, R. (1964) *J. Biol. Chem. 239*, 2370−2378.
53. Wells, A. V., Li, P., Champion, P. M., Martinis, S. A., and Sligar, S. G. (1992) *Biochemistry 31*, 4384−4393.
54. Davydov, D. R., Knyushko, T. V., and Hui Bon Hoa, G. (1992) *Biochem. Biophys. Res. Commun. 188*, 216−221.
55. Imai, Y., and Sato, R. (1967) *Eur. J. Biochem. 1*, 419−426.
56. Ristau, O., Rein, H., Greschner, S., Janig, G. R., and Ruckpaul, K. (1979) *Acta Biol. Med. Ger. 38*, 177−185.
57. Graham-Lorence, S. E., and Peterson, J. A. (1996) *FASEB J. 10*, 206−214.
58. Poulos, T. L. (1995) *Curr. Opin. Struct. Biol. 5*, 767−774.
59. Park, S. Y., Shimizu, H., Adachi, S., Nakagawa, A., Tanaka, I., Nakahara, K., Shoun, H., Obayashi, E., Nakamura, H., Iizuka, T., and Shiro, Y. (1997) *Nature Struct. Biol. 4*, 827−832.
60. Okamoto, N., Imai, Y., Shoun, H., and Shiro, Y. (1998) *Biochemistry 37*, 8839−8847.
61. Kundrot, C. E., Ponder, J. W., and Richards, F. M. (1998) *J. Comput. Chem. 12*, 402−409.
62. Cabani, S., Gianni, P., Mollica, V., and Lepori, L. (1981) *J. Solution Chem. 10*, 563−595.
63. Paulsen, M. D., and Ornstein, R. L. (1995) *Proteins 21*, 237−243.
64. Khan, K. K., Mazumdar, S., Modi, S., Sutcliffe, M., Roberts, G. C., and Mitra, S. (1997) *Eur. J. Biochem. 244*, 361−370.
65. Modi, S., Primrose, W. U., Boyle, J. M., Gibson, C. F., Lian, L. Y., and Roberts, G. C. (1995) *Biochemistry 34*, 8982−8988.
66. Modi, S., Sutcliffe, M. J., Primrose, W. U., Lian, L. Y., and Roberts, G. C. K. (1996) *Nature Struct. Biol. 3*, 414−417.
67. Helms, V., Deprez, E., Gill, E., Barret, C., Hoa, G. H. B., and Wade, R. C. (1996) *Biochemistry 35*, 1485−1499.

BI981397A